Eur. Phys. J. B (2013) 86: 121
DOI: 10.1140/epjb/e2013-31003-y

THE EUROPEAN PHYSICAL JOURNAL B

Regular Article

# Temperature dependent exchange bias effect in polycrystalline $BiFeO_3$/FM (FM = NiFe, Co) bilayers

Xiaobo Xue[1], Xueyong Yuan[2], Wenbin Rui[1], Qingyu Xu[2,a], Biao You[1], Wei Zhang[1], Shiming Zhou[3], and Jun Du[1,b]

[1] National Laboratory of Solid State Microstructures and Department of Physics, Nanjing University, Nanjing 210093, P.R. China
[2] Department of Physics, Southeast University, Nanjing 211189, P.R. China
[3] Department of Physics, Tongji University, Shanghai 200092, P.R. China

Received 3 November 2012 / Received in final form 23 January 2013
Published online 27 March 2013 – 

**Abstract.** Extensive studies on the temperature ($T$) dependent exchange bias effect were carried out in polycrystalline $BiFeO_3$(BFO)/NiFe and BFO/Co bilayers. In contrast to single-crystalline BFO/ferromagnet (FM) bilayers, sharp increase of the exchange bias field ($H_E$) below 50 K were clearly observed in both of these two bilayers. However, when $T$ is higher than 50 K, $H_E$ increases with $T$ and decreases further when $T$ is larger than 230 K (for BFO/NiFe) or 200 K (for BFO/Co), which is similar to those reported in single-crystalline BFO/FM bilayers. After the exploration of magnetic field cooling, the temperature dependent exchange bias can be explained considering two contributions from both the interfacial spin-glass-like frustrated spins and the polycrystalline grains in the BFO layer. Moreover, obvious exchange bias training effect can be observed at both 5 K and room temperature and the corresponding results can be well fitted based on a recently proposed theoretical model taking into account the energy dissipation of the AFM layer.

## 1 Introduction

Nowadays, exchange bias (EB) in ferromagnet (FM)/antiferromagnet (AFM) bilayer is widely used in spintronic devices [1]. Electric field tunable EB with much lower power consumption is very likely to be realized in the next generation spintronic devices if a room temperature multiferroic material can be taken as AFM layer [2]. $BiFeO_3$ (BFO) may be such a promising candidate due to both ferroelectric and antiferromagnetic phase transition temperatures well above room temperature [3,4]. Considering $G$-type AF structure of BFO, the (001), (110) surfaces are all fully compensated, which should give rise to no EB [5]. However, significant EB effect has been observed in a variety of BFO/FM bilayers, such as BFO/NiFe [6], BFO/Co [7], BFO/CoFe [8], BFO/CoFeB [9], BFO/$LaSrMnO_3$ [10], BFO/$Fe_3O_4$ [11] and so on. In these bilayers, the EB is generally considered to be resulted from the interfacial pinned uncompensated spins near the BFO/FM interface, which may arise from magnetic heterogeneities [8], Dzyaloshinskii-Moriya (DM) interaction [12], electronic orbital reconstruction [10,11] etc.

In most of the EB studies on BFO/FM bilayers, epitaxially grown single crystalline BFO films were employed to achieve sizeable exchange bias field ($H_E$). In fact, polycrystalline exchange biased bilayers are much more useful in application due to low-cost and convenient fabrication. However, EB in polycrystalline BFO/FM systems has rarely been studied [13,14]. No matter the BFO layer is single- or polycrystalline, to our knowledge, only very few studies were carried out concerning about the temperature dependent EB effect in BFO/FM bilayers, especially at low temperature region [7,8,10,11]. Naganuma et al. [7] reported that in CoFe/BFO (001) bilayers, $H_E$ increases between 10 to 250 K and disappears at 390 K, i.e. the so-called blocking temperature $T_B \sim 390$ K, while $H_C$ decreases monotonically from 10 to 390 K. In another work also carried out in CoFe/BFO bilayer [8], although the authors claimed that $H_E$ exhibits very little temperature dependence from 5 K to 300 K, we notice that besides $H_C$ decreasing monotonically in the entire temperature region, $H_E$ decreases slowly from 250 K to 50 K with decreasing $T$ and then levels off when $T$ is below 50 K. For both of these above experiments, metallic magnetic alloy was served as FM layer and EB could be easily obtained at room temperature. However, if magnetic oxides are chosen as FM layer, the temperature dependent EB will be quite different. Yu et al. [10] successfully made fully epitaxial BFO/$La_{0.7}Sr_{0.3}MnO$ bilayers and found that $H_E$ decreased monotonically with increasing $T$ and disappeared at about 100 K, i.e. $T_B \sim 100$ K, which is much lower than the Néel temperature $T_N$ ($\sim$640 K) of bulk BFO [3]. The similar temperature dependence of EB with also much

[a] e-mail: xuqingyu@seu.edu.cn
[b] e-mail: jdu@nju.edu.cn

lower $T_B$ of about 200 K was observed in single-crystalline BFO/$Fe_3O_4$ heterostructures [11].

Up to date, the study on temperature dependent EB in polycrystalline BFO/FM bilayers is still lacking. The fundamental difference between polycrystalline and epitaxial BFO films is that the latter has a homogeneous exchange stiffness with the possible formation of AF domains whereas the former exhibits an uncoupled grain behavior wherein each grain can be considered as single domain with no interaction with the neighboring grains [15]. In this presented work, extensive studies on temperature dependent EB were carried out in polycrystalline BFO/NiFe and BFO/Co bilayers wherein BFO layer are single-phase polycrystalline. In contrast to the single-crystalline BFO/FM bilayers, a major difference of sharp increase of $H_E$ below 50 K can be observed clearly, which may be due to interfacial spin-glass pinning behavior.

## 2 Experimental

Polycrystalline BFO (40 nm)/NiFe (3.6 nm) and BFO (40 nm)/Co (4 nm) bilayers were fabricated by pulsed laser deposition (PLD) combined with magneto-sputtering technique. After the BFO film was deposited by PLD, the samples were transferred to a sputtering chamber for FM (NiFe or Co) layer deposition, during which a magnetic field of 150 Oe was applied to induce unidirectional and uniaxial anisotropies. X-ray diffraction (XRD) and transmission electron microscopy (TEM) results show that the BFO films with varied thickness from 8 nm to 240 nm are all single-phase polycrystalline in $R$-3c structure (PDF#88-0633) and any impurity phases are absent. Detailed description of the sample preparation procedure and the corresponding structure characterization can be found in reference [14].

Temperature dependent magnetic properties of these bilayers were measured by a commercial SQUID-VSM (Quantum Design) from 5 K to 300 K. In order to obtain accurate values of $H_E$ and $H_C$, cares were taken to minimize the residual magnetic field to almost zero before measurements. A commercial vibrating sample magnetometer (VSM, Microsense EV7) was employed to measure the magnetic hysteresis ($M$-$H$) loops at temperatures higher than 300 K. Exchange bias training effect was also detected in the bilayer samples by measuring the $M$-$H$ loop continuously. The typical time interval between two consecutive $M$-$H$ loops is about 15 min and 10 min when the measuring temperature is kept at 5 K and 300 K, respectively.

## 3 Results and discussion

Before measuring the temperature dependent $M$-$H$ loops, the sample was cooled from room temperature to 5 K under zero magnetic field (ZFC) or a certain magnetic field (FC). After the temperature is stable, more than five cycles are performed, which can reduce the influence of training effect remarkably. After that, $M$-$H$ loops were measured at some specific elevated temperatures. During the heating process between two measuring temperatures, the magnetic field was kept zero. Figure 1 shows the ZFC $M$-$H$ loops at several representative temperatures for BFO/NiFe bilayer. In Figure 1d, obvious exchange bias effect can be observed at room temperature with the full loop shifted to the negative magnetic field side. As the temperature is decreased, both the exchange bias field ($H_E$) and the coercivity ($H_C$) change significantly. When the temperature reaches 5 K (Fig. 1a), although $H_E$ does not change too much compared with that at 300 K, $H_C$ increases significantly, leading to the $M$-$H$ loop not shifted to the negative side completely. In addition, all the $M$-$H$ loops at various temperatures show relatively large squareness. Much similar result can be also found in BFO/Co bilayer (not shown here), which shows relatively larger $H_E$ and $H_C$ values at all temperatures and this may be due to larger strength of interfacial exchange coupling between BFO and Co layers.

The overall temperature dependences of $H_E$ and $H_C$ from 5 K to 300 K for the above two bilayers are similar and displayed in Figure 2, showing interesting and surprising features. As $T$ is decreased from 300 K, $H_E$ increases initially and reaches a maximum when $T$ is about 230 K (for BFO/NiFe) or 200 K (for BFO/Co). After that, $H_E$ keeps decreasing and reaches a minimum when $T$ is decreased to about 50 K. When $T$ is decreased further, $H_E$ increases abruptly. However, in the measuring temperature range from 300 K to 5 K, $H_C$ always increases monotonically with decreasing $T$. Compared with that at 300 K, the value of $H_C$ at 5 K is enhanced about ten times for BFO/NiFe and five times for BFO/Co bilayers, respectively. When $T$ is larger than 300 K, according to the $M$-$H$ loops measured by VSM (not shown here), both $H_E$ and $H_C$ decrease monotonically with increasing $T$ and $H_E$ becomes zero when $T$ is about 400 K, i.e. the blocking temperature $T_B \sim 400$ K, which is consistent with that obtained in CoFe/BFO (001) bilayer [7]. This value is much smaller than the Néel temperature of BFO, which may be due to severe interface diffusion and/or reaction between BFO and FM layers [16].

Figure 2 unambiguously shows that there is a sharp increase below 50 K on the $H_E \sim T$ curve for both BFO/NiFe and BFO/Co bilayers, which was never reported before in single-crystalline BFO/FM bilayers. However, in comparison with the temperature dependent EB in single-crystalline BFO/FM bilayers [7,8], it is in common that $H_E$ increases with $T$ when $T$ is higher than about 50 K and acquires maximum when $T$ is between 200 and 250 K. This feature was absent in conventional exchange biased FM/AFM system, in which both $H_E$ and $H_C$ always increase with decreasing $T$ and it can be explained in terms of enhanced uniaxial and unidirectional anisotropies at low temperature range [17]. Although the anomalous temperature variation behavior in BFO/FM bilayers has not been explained thoroughly yet, Naganuma et al. [7] considered that it may be due to temperature

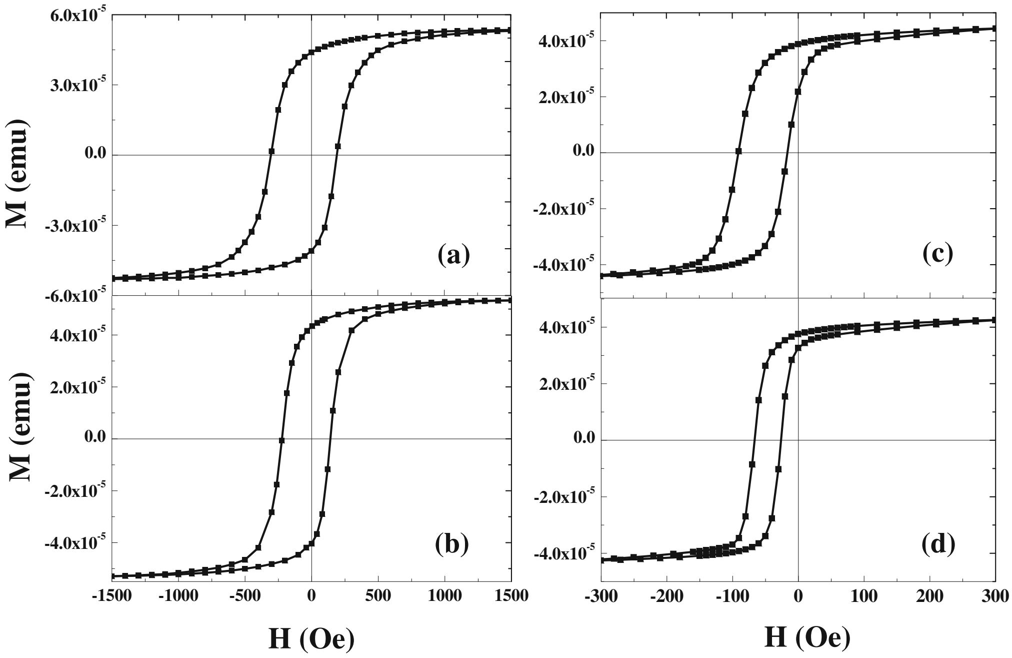


**Fig. 1.** Zero-field-cooled $M$-$H$ loops at $T = 5$ K (a), 50 K (b), 230 K (c) and 300 K (d) for BFO (40 nm)/NiFe (3.6 nm) bilayer sample.

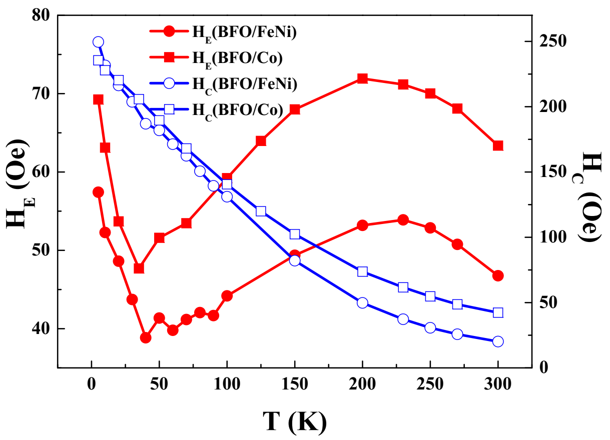


**Fig. 2.** Temperature dependences of zero-field-cooled $H_E$ and $H_C$ in the bilayer samples of BFO (40 nm)/NiFe (3.6 nm) and BFO (40 nm)/Co (4.0 nm), respectively.

dependence of ferroelectric (FE) domains through magnetoelectric (ME) coupling effect. We conjecture that the size or the polarization direction of the FE domain in the BFO layer will be changed as $T$ is decreased. This will result in change of the AFM domains because the FE and AFM domains are coupled through ME effect, leading to $H_E$ varying with $T$, accordingly [18].

We now turn to discuss the issue of sharp increase of $H_E$ when $T$ is below about 50 K. In conventional polycrystalline FM/AFM bilayers, e.g. CoFe/IrMn, NiFe/FeMn or NiFe/CoO, sometimes one can observe low-$T$ sharp increase of $H_E$ [19,20], which is attributed to disordered or frustrated interfacial FM/AFM spins forming spin-glass-like phases at low temperature. Exchange bias in spin-glass/FM bilayer was first observed in CuMn/Co bilayer [21] and soon after in FeAu/NiFe bilayer [22], in which CuMn and FeAu are well-known canonical spin-glass systems. For the FM/AFM bilayers, a gradual freezing of the interfacial frustrated spins at low $T$, typically between 4 and 70 K, has been used to explain the low-$T$ sharp increase of $H_E$ [23]. These frustrated spins may come from interfacial roughness, structural defects, interlayer mixing or diffusion and so on. As for the high-$T$ exchange bias effect, it is ascribed to the AFM grains themselves. Therefore, in these EB systems, the $T_B$ distribution presents a bimodal character, with a high-$T$ contribution attributed to AFM grains and low-$T$ contribution ascribed to interfacial spin-glass-like phases [23]. Very recently, this bimodal $T_B$ distribution has been reported in BFO/CoFeB bilayer with epitaxially BFO layer grown on $SrTiO_3$ (001) substrate, in which the low-$T$ contribution is resulted from frustrated spins formatted by in-plane reorientation of BFO uncompensated spins [15].

In order to further investigate the relationship between the occurrence of sharp increase of $H_E$ below 50 K and the formation of interfacial spin-glass-like phases, magnetic field cooling (FC) was done in the BFO/NiFe bilayer sample. The sample was cooled under 7 T from 300 K to 5 K, after that the $M$-$H$ loops were recorded at some specific elevated temperatures as those done after ZFC process. Then the asymmetry along the $M$ axis has been extracted out for each $M$-$H$ loop, which is represented by $\Delta M$ and its temperature dependence is displayed in Figure 3a. Here, $\Delta M$ means the difference between the magnetic moments at positive and negative saturation

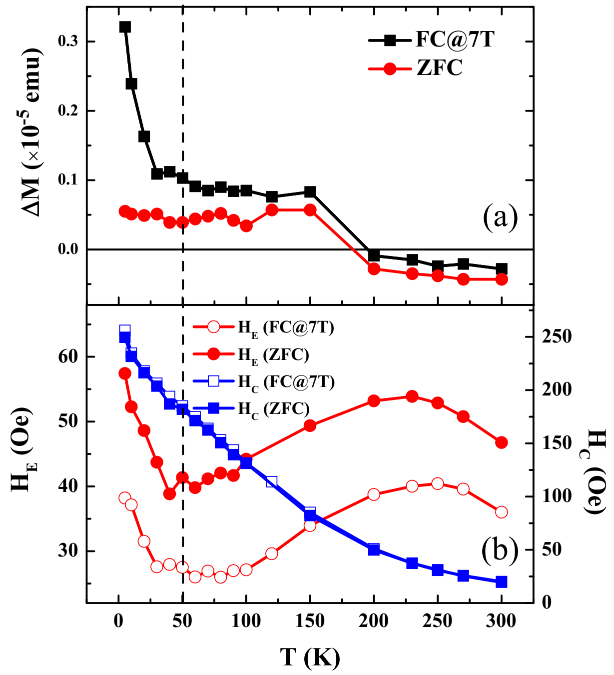


**Fig. 3.** Zero-field-cooled and field-cooled temperature dependences of (a) $\Delta M$, and (b) $H_E$ and $H_C$ for BFO (40 nm)/NiFe (3.6 nm) bilayer sample.

states. Figure 3a provides the comparison of $\Delta M$ before and after field cooling. It can be seen that after field cooling $\Delta M$ increases generally in the entire measuring temperature region. More remarkably, the $\Delta M$ increases significantly when $T$ is below 50 K, suggesting a large amount of interfacial frustrated spins frozen and aligned to the cooling field direction, which may form spin-glass-like phases at this low-$T$ region. The increase of $\Delta M$ below 50 K also means weakening of the frozen states after 7 T field cooling. Because this variation behavior of $\Delta M$ is much similar to that of $H_E$ at the same temperature range, it is reasonable to infer that they are attributed from the same origin, i.e. the interfacial spin-glass-like phases. As for the value of $\Delta M$ for FC generally larger than that for ZFC when $T$ is larger than 50 K, it may be resulted from some other interfacial spin-glass-like phases, which may even exist at about 250 K [24].

Therefore, in the presented polycrystalline BFO/FM bilayers, the exchange bias effect may come from two sources. One is the polycrystalline BFO grains, which mainly dominate the EB at high-$T$ region where $T$ is larger than 50 K. The other is interfacial frustrated spins, which mainly dominates the EB below 50 K. The corresponding high-resolution transmission electron microscopy (HRTEM) image for BFO/NiFe bilayer can be found in Figure 3d in reference [14], which shows that the interface between NiFe and BFO is not very flat with interface roughness evaluated to be about 2 nm. In addition, interface diffusion or reaction between BFO and FM layers is inevitable. These factors are likely to result in formation of interfacial frustrated spins and spin-glass-like phases below room temperature. When the BFO layer is very thin, the interfacial contribution may be dominant and thus result in sharp increase of $H_E$ at low-$T$ region.

After field cooling, besides $\Delta M$, $H_E$ also changes significantly. For comparison, the temperature dependent $H_E$ and $H_C$ after FC and ZFC processes are displayed in Figure 3b. It shows clearly that the $H_E \sim T$ plot shifts down remarkably while the $H_C \sim T$ plot keeps almost unchanged after FC. To our knowledge, BFO has a very high $T_N$ (ca. 640 K [3]), which will not result in significant change of $H_E$ if the FC procedure is operated from 300 K. However, because of the potential problem of interface reaction [25], the conventional method of inducing unidirectional anisotropy by magnetic-field annealing through $T_N$ is infeasible in BFO/FM bilayers. Usually, just like we did in this presented work, the bilayer is deposited under an applied magnetic field. During the deposition of FM layer on top of BFO, the AFM domains in BFO are probably rearranged to minimize the total energy under external magnetic field and then results in an effective exchange imbalance at the interface and an exchange bias, accordingly [6,25]. Such a rearrangement of AFM domains is relatively easy for imperfectly antiparallel spins as in BFO, which will not lead to a stable EB on the FM layer [6]. On the other hand, in the presented BFO/FM bilayers, the BFO layer is very thin (40 nm) with polycrystalline structure, possibly including some quite small grains with their $T_N$ much lower than bulk one. We conjecture that these factors may cause irreversible change of the AFM domains in the BFO layer after 7 T field cooling from 300 K to 5 K, leading to decrease of interfacial pinned uncompensated AFM spins and then reducing $H_E$ consequently. It was reported that the fraction of pinned uncompensated spins responsible for EB can be just a small fraction (a few percent) of the entire surface spins [8], the other spins responsible for $H_C$ enhancement may not change too much after FC, leading to almost the same temperature dependence of $H_C$ as that of ZFC.

The exchange bias training effect is also very interesting in single-crystalline BFO based bilayers. In most of the studies, no significant training effect was observed, which means that $H_E$ and $H_C$ keep almost the same with varying the magnetic cycle number $n$ [6,26]. However, up to date, the EB training results have not been reported in polycrystalline BFO based bilayers. Figures 4a and 4b show the variation of $H_E$ and $H_C$ along with $n$ at both 300 K and 5 K, respectively in BFO/NiFe bilayer. It exhibits that obvious training effect can be observed at both temperatures and it behaves quite differently at these two temperatures. At 300 K, both $H_E$ and $H_C$ change slowly with $n$. However, at 5 K, both $H_E$ and $H_C$ change abruptly between $n = 1$ and $n = 2$, and approaches stable very soon after $n$ is larger than 2. We think that at the interface between FM and polycrystalline BFO, there are still some unstable AFM spins responsible for EB, which will be rearranged and eventually approach to equilibrium state under magnetic cycles. However, the relaxation process is quite fast at low temperature and very slow at room temperature. Very surprisingly, the present EB training results cannot be well fitted by an empirical $n^{-1/2}$ law, which

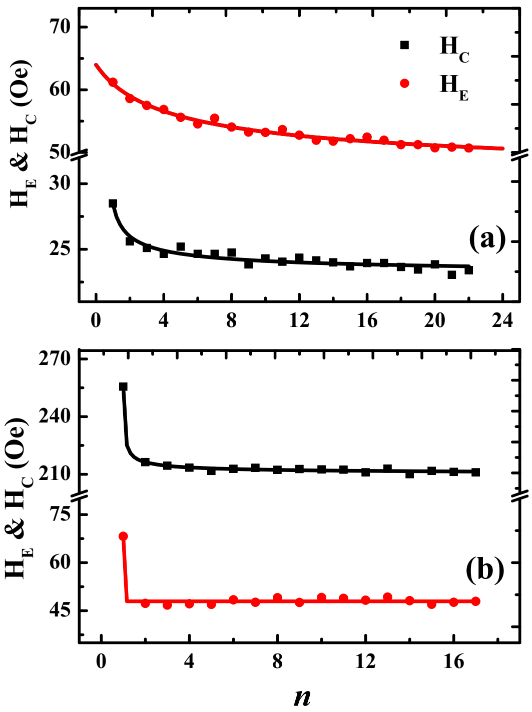


**Fig. 4.** The variation of zero-field-cooled $H_E$ and $H_C$ along with the cycle number $n$ at 300 K (a), and 5 K (b) for BFO (40 nm)/NiFe (3.6 nm) bilayer sample. The dots and lines represent the experimental and fitted results, respectively.

is often satisfied in conventional FM/AFM bilayers with $n > 1$. Very recently, Su and Hu [27] proposed a power-law function describing EB training effect as

$$H_E(n) = H_E(\infty) + k_1(n + n_0)^{-1/2} \quad (1)$$

$$H_C(n) = H_C(\infty) + k_2(n + n_0')^{-1/2} \quad (2)$$

where $H_{E,C}(\infty)$, $k_1$, $k_2$, $n_0$ and $n_0'$ are the fitting parameters. These analytical functions are obtained by introducing the out-of-step of energy dissipation and Landau-Lifshitz-Gilbert (LLG) equation and the authors claim that the energy dissipation pattern of the AFM plays a crucial role in the EB training effect. To our understanding, this kind of EB training effect can be categorized as thermal activation [28] and not Hoffmann athermal one [29]. By using the power-law functions given in equations (1) and (2), the $n$ dependence of $H_E$ and $H_C$ in the polycrystalline BFO/NiFe bilayer can be well fitted at both 5 K and 300 K, as displayed by the lines in Figures 4a and 4b. All the fitting parameters can be found in Table 1, which also indicates that $H_E$ and $H_C$ arrive at equilibrium state very quickly at 5 K and very slowly at 300 K. In other samples, e.g. the FM layer is changed to Cobalt or the thickness of the BFO layer is changed to 80 nm, the EB training results can also be well fitted by using equations (1) and (2), indicating thermal activated EB training effect generally existing in polycrystalline BFO/FM bilayers.

**Table 1.** Fitting parameters of exchange bias training effect at both 300 K and 5 K in zero-field-cooled BFO (40 nm)/NiFe (3.6 nm) bilayer sample.

| $T = 300$ K | | | $T = 5$ K | | |
|---|---|---|---|---|---|
| $H_E(\infty)$ (Oe) | $k_1$ (Oe) | $n_0$ | $H_E(\infty)$ (Oe) | $k_1$ (Oe) | $n_0$ |
| 44.84 | 29.78 | 2.41 | 47.93 | 0.00154 | –1 |
| $H_C(\infty)$ (Oe) | $k_2$ (Oe) | $n_0'$ | $H_C(\infty)$ (Oe) | $k_2$ (Oe) | $n_0'$ |
| 22.90 | 3.72 | –0.55 | 209.8 | 0.55 | –0.98 |

## 4 Conclusions

To summarize, temperature dependent exchange bias effect was extensively investigated in polycrystalline BFO/NiFe and BFO/Co bilayer samples and sharp increase of $H_E$ below 50 K was unambiguously observed. After the bilayer samples were cooled under a magnetic field of 7 T, $H_E$ decreases significantly whereas $H_C$ keeps almost unchanged in the whole measuring temperature from 5 K to 300 K. These above exchange bias phenomena can be understood by considering two contributions both from the interfacial frustrated spins which can generate spin-glass-like phases and polycrystalline BFO grains in the BFO layer. Obvious exchange bias training effect was observed at both low temperature and room temperature. The corresponding variation of $H_E$ and $H_C$ along with the cycle number are compared at 5 K and 300 K and can be well fitted by power-law functions within the framework considering energy dissipation of the AFM layer.

This work was supported by National Basic Research Program of China (Nos. 2010CB923401 and 2010CB923404), National Science Foundations of China (Nos. 11074112, 11174131, 10974087 and 51172044), and National Science Foundation of Jiangsu Province of China (BK2011617).

## References


1. B. Dieny, V.S. Speriosu, S.S.P. Parkin, B.A. Gurney, D.R. Wilhoit, D. Mauri, Phys. Rev. B **43**, 1297 (1991)
2. M. Bibes, A. Barthélémy, Nat. Mater. **7**, 425 (2008)
3. J.R. Teague, R. Gerson, Solid State Commun. **8**, 1073 (1970)
4. S.V. Kiselev, R.P. Ozerov, G.S. Zhdanov, Sov. Phys. Dokl. **7**, 742 (1963)
5. F.M. Bai, G. Yu, Y.C. Wang, L.C. Jin, H.Z. Zeng, X.L. Tang, Z.Y. Zhong, H.W. Zhang, Appl. Phys. Lett. **101**, 092401 (2012)
6. J. Dho, M.G. Blamire, J. Appl. Phys. **106**, 073914 (2009)
7. H. Naganuma, M. Oogane, Y. Ando, J. Appl. Phys. **109**, 07D736 (2011)
8. L.W. Martin, Y.H. Chu, M.B. Holcomb, M. Huijben, P. Yu, S.J. Han, D. Lee, S.X. Wang, R. Ramesh, Nano Lett. **8**, 2050 (2008)
9. D. Lebeugle, A. Mougin, M. Viret, D. Colson, J. Allibe, H. Béa, E. Jacquet, C. Deranlot, M. Bibes, A. Barthélémy, Phys. Rev. B **81**, 134411 (2010)
10. P. Yu, J.-S. Lee, S. Okamoto, M.D. Rossel, M. Huijben, C.-H. Yang, Q. He, J.X. Zhang, S.Y. Yang, M.J. Lee, Q.M. Ramasse, R. Erni, Y.-H. Chu, C.-C. Kao, L.W. Marin, R. Ramesh, Phys. Rev. Lett. **105**, 027201 (2010)

11. T.L. Qu, Y.G. Zhao, P. Yu, H.C. Zhao, S. Zhang, L.F. Yang, Appl. Phys. Lett. **100**, 242410 (2012)
12. S. Dong, K. Yamaguchi, S. Yunoki, R. Yu, S. Liang, A. Moreo, J.-M. Liu, S. Picozzi, E. Dagotto, Phys. Rev. Lett. **103**, 127201 (2009)
13. T. Hauguel, S.P. Pogossian, D.T. Dekadjevi, D. Spenato, J.P. Jay, M.V. Indenborn, J.B. Youssef, J. Appl. Phys. **110**, 073906 (2011)
14. X.Y. Yuan, X.B. Xue, X.N. Zhang, W. Zheng, M. Yang, J. Du, D. Wu, Q.Y. Xu, Solid State Commun. **152**, 241 (2012)
15. C.K. Safeer, M. Chamfrault, J. Allibe, C. Carretero, C. Deranlot, E. Jacquet, J.-F. Jacquot, M. Bibes, A. Bathélémy, B. Dieny, H. Béa, V. Baltz, Appl. Phys. Lett. **100**, 072402 (2012)
16. T. Yu, H. Naganuma, W.X. Wang, Y. Ando, X.F. Han, J. Appl. Phys. **111**, 07D908 (2012)
17. S.N. Dong, Y.P. Yao, Y. Hou, Y.K. Liu, Y. Tang, X.G. Li, Nanotechnology **22**, 385701 (2011)
18. H. Béa, M. Bibes, F. Ott, B. Dupé, X.–H. Zhu, S. Petit, S. Fusil, C. Deranlot, K. Bouzehouane, A. Barthélémy, Phys. Rev. Lett. **100**, 017204 (2008)
19. L.E. Femandez-Outon, G. Vallejo-Fernandez, S. Manzoor, B. Hillebrands, L. O'Grady, J. Appl. Phys. **104**, 093907 (2008)
20. K. Takano, R.H. Kodama, A.E. Berkowitz, W. Cao, G. Thomas, Phys. Rev. Lett. **79**, 1130 (1997)
21. M. Ali, P. Adie, C.H. Marrows, D. Greig, B.J. Hickey, R.L. Stamps, Nat. Mater. **6**, 70 (2007)
22. F.T. Yuan, J.K. Lin, Y.D. Yao, S.F. Lee, Appl. Phys. Lett. **96**, 162502 (2010)
23. V. Baltz, B. Rodmacq, A. Zarefy, L. Lechevallier, B. Dieny, Phys. Rev. B **81**, 052404 (2010)
24. B. Ramachandran, M.S.R. Rao, Appl. Phys. Lett. **95**, 142505 (2009)
25. J. Dho, X.D. Qi, H. Kim, J.L. MacManus-Driscoll, M.G. Blamire, Adv. Mater. **18**, 1445 (2006)
26. L.W. Martin, Y.H. Chu, Q. Zhan, R. Ramesh, S.J. Han, S.X. Wang, M. Warusawithana, D.G. Schlom, Appl. Phys. Lett. **91**, 172513 (2007)
27. Y.C. Su, J.G. Hu, J. Appl. Phys. **112**, 043906 (2012)
28. M.K. Chan, J.S. Parker, P.A. Crowell, C. Leighton, Phys. Rev. B **77**, 014420 (2008)
29. A. Hoffmann, Phys. Rev. Lett. **93**, 097203 (2004)